

Electron-impact excitation of holmium atoms

Yu M Smirnov

Abstract. The electron-impact excitation of holmium atoms was studied by the method of extended crossing beams. The cross sections and the optical excitation functions were obtained for odd levels of Ho I, including the 22014 cm^{-1} laser level. Over 99% of the atoms were shown to reside in the ground level prior to collisions with electrons. Also measured were the excitation cross sections for six even levels, which presumably participate in the formation of inversion population in a gas-discharge holmium vapour laser.

1. Introduction

The generation in gas lasers involving transitions in atoms and singly charged ions of rare-earth elements (REEs) was obtained during the first years following the discovery of lasers [1, 2]. During that time, pulsed lasing was demonstrated on transitions in samarium, europium, thulium, and ytterbium atoms [3]. During the ensuing years, the laser lines arising from transitions in REEs grew significantly in number. However, all of them still belonged to the four above-listed elements.

The most important factor which determines, in principle, the feasibility of obtaining lasing on transitions of a specific atom or ion is the electron shell structure of this particle: the energy level diagram and quantum characteristics of the levels, possible transitions between the levels, transition probabilities and radiative lifetimes, etc. From this viewpoint, standing out among the REEs are, for instance, europium and ytterbium, in which the lowest excited levels are separated from the ground level by an energy gap exceeding 12000 cm^{-1} . However, in this respect, the samarium atom is much closer to neodymium or gadolinium than to europium or ytterbium and possesses a large group of low-lying levels [4].

Another possible reason for this historically established situation may lie with a rather high pressure of Sm, Eu, Tm, and Yb vapour at relatively moderate temperatures. Fig. 1 shows the temperature dependence of the saturation vapour pressure for several elements, including the REEs; the basis for Fig. 1 was provided by Fig. 13.15c from Ref. [5]. One can see that all REEs are clearly subdivided into two groups: the elements with low (Yb, Eu, Sm, Tm) and

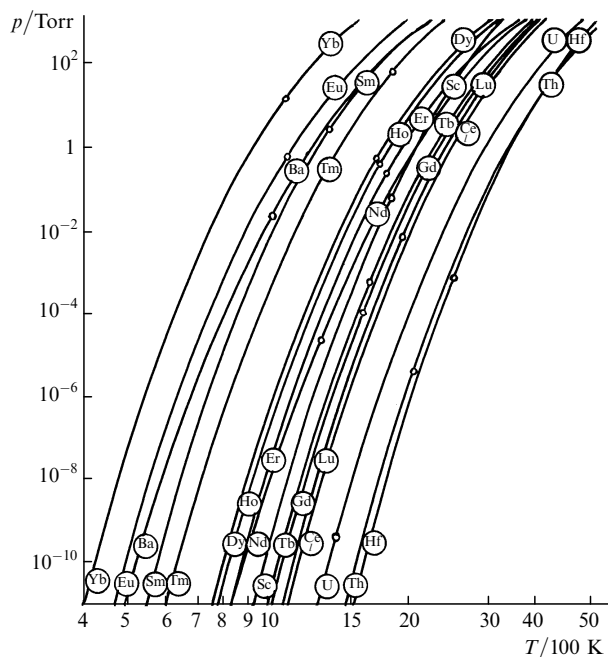


Figure 1. Temperature dependences of the saturation vapour pressure of elements [5]: small circles denote melting points and *l* signifies the liquid phase.

medium (Dy, Ho, Er, Nd, Tb, Gd, Lu, Ce) vaporisation temperatures. Also falling into the latter group are praseodymium and promethium not shown in Fig. 1. A temperature *t* for which the saturation vapour pressure of an element amounts to 0.1 Torr can be treated as a conventional boundary as was done in Ref. [3]. For the four elements of the first group this temperature proves to be below $1000\text{ }^{\circ}\text{C}$ (owing to a misprint in Ref. [3], gadolinium supposedly falls into the same group with the alleged temperature of $809\text{ }^{\circ}\text{C}$, whereas the actual value is $1809\text{ }^{\circ}\text{C}$). The corresponding temperature for the remaining REEs falls in the $1300\text{--}2000\text{ }^{\circ}\text{C}$ range.

The temperature barrier between the two groups was overcome quite recently: Gerasimov [6] reported attaining the laser oscillation on one of the atomic transitions of holmium. A tube of beryllium oxide employed as a gas-discharge channel could be heated to $1650\text{ }^{\circ}\text{C}$, which corresponds to a saturation vapour pressure of holmium of about 2 Torr. The lasing was observed in the $1300\text{--}1600\text{ }^{\circ}\text{C}$ temperature range (holmium vapour pressure in the range 0.1–1.1 Torr) at a line with a wavelength $\lambda = 1032 \pm 0.5\text{ nm}$. This line was assigned to the transition from the 22014 cm^{-1} level to the 12344 cm^{-1} level. The lower

Yu M Smirnov Moscow Power Institute (Technical University),
Krasnokazarmennaya ul. 14, 111250 Moscow, Russia

Received 12 January 2000

Kvantovaya Elektronika 30 (6) 545–550 (2000)

Translated by E N Ragozin, edited by M N Sapozhnikov

level was classified as $4f^{10}(^5I_7)5d_{3/2}6s^2(7,3/2)_{13/2}$ in terms of J_1j coupling and the upper one as $4f^{11}(^4I^o)5d6s(^3D)_{15/2}^o$ in terms of LS coupling. The upper level was not identified because it is strongly mixed; the main component (30%) is $^4I^o$, while the leading admixture component ($^4I^o$)(3D) $^2K^o$ amounts to 27%, with the total contribution of the remaining admixture components accounting for about 43% [7]. Therefore, lasing on the above-specified transition is effected by the $4f \rightarrow 6s$ conversion, which is forbidden in a regular LS-coupling scheme.

As noted in Ref. [6], ‘the spectrum of holmium is one of the least explored among the REEs.’ Wyart et al. [8] classified 913 lines of Ho I out of 1462 lines recorded in their notable paper, thereby making a significant contribution to the list of previously known levels of atomic holmium. However, this publication did not change the classification situation of the Ho I spectrum in the visible region because Wyart et al. [8] explored the IR region from 2493 to 12344 cm^{-1} . More recently [9], four lines of Ho I were classified and three new energy levels were determined. Nevertheless, Gerasimov’s remark [6] that the holmium spectrum is poorly known still holds.

This fact engaged the attention of the author when there arose a demand for classifying a large number of spectral lines of atomic and singly charged holmium in studies of inelastic electron-atom collisions. The results obtained in this case are outlined in Ref. [10]. Also discussed in Ref. [10] are the basic principles of classification with recourse to the data obtained in studies of excitation of atoms and ions by monoenergetic electron.

The atomic constants of Ho I and Ho II are known even less than their spectra. The radiative transition probabilities A_{ki} for 25000 spectral lines in the spectra of 70 elements were determined in a well-known monograph [11]. However, only three A_{ki} probabilities for atomic holmium and none of those for its singly charged ion are found in Ref. [11]. More recently [12], the multichannel delayed coincidence method was used to measure the lifetimes of 12 Ho I levels and two Ho II levels. Also determined were the oscillator strengths of 29 atomic spectral lines and of four spectral lines of the singly charged holmium ion. Comparatively recently [13], measurements were made of the lifetimes of three HoII levels, one of which had been studied in Ref. [12], and three A_{ki} probabilities were determined.

The excitation cross sections for the spectral lines of Ho I were first measured in Ref. [14], with their scale based on the excitation cross sections of the molecular nitrogen ion as the reference. Subsequently, a changeover to the more trustworthy helium reference was made, for which the excitation cross sections were determined with a high accuracy in Ref. [15]. The new results obtained on this basis for HoII were published in Ref. [16]. The cross section scales determined with reference to nitrogen and helium differ by nearly a factor of three.

As stated by Gerasimov [6] in the consideration of the conditions for lasing, ‘the upper laser level has the same parity as the ground state and cannot be excited directly by electron impact in a discharge.’ However, this statement is not entirely legitimate. The parity selection rule is rather rigorous for the majority of radiative transitions in atoms and ions (especially so for those with a comparatively small nuclear mass). Upon excitation by electron impact, however, it shows up not in the form of a rigorous prohibition but only as a factor to somewhat reduce the excitation cross sections in comparison with the allowed ones.

This work is concerned with the excitation of the energy levels of holmium atoms whose parity coincides with the parity of the ground level and, hence, with that of the laser level of Ho I. In this case, selected from the extensive data are primarily those transitions for which the optical excitation functions (OEFs) were recorded.

2. Experimental

The method of extended crossing beams was used, as in Refs [14–16]. In the present work, it is not expedient to outline the principles of this method and the instrumentation, which were repeatedly discussed earlier (most thoroughly in Ref. [17]).

Starting from the objectives of this work, the possibility of thermal population of the low-lying levels of atomic holmium upon its vaporisation should be treated as the most significant factor. The heating of holmium was accomplished by direct exposure of the metal surface to an electron beam. The saturation vapour pressure of holmium at its melting temperature is quite high (see Fig. 1), and therefore a rather dense atomic beam can easily be obtained through vaporisation of holmium from the solid phase. For a temperature of the metal surface of 1550 K, the atomic density in the region of intersection of the atomic and electron beams was $1.2 \times 10^{10} \text{ cm}^{-3}$. Despite the fact that this value was five times lower than the value obtained in the experiment in Ref. [14], optimising the operation of all the systems of our facility furnished a more extensive and reliable information.

The potentials of contemporary techniques do not permit the density of excited holmium atoms to be measured directly in the primary beam. Assuming that the thermodynamic equilibrium takes place, an estimate gives the following populations of low-lying levels of Ho I (in percentage of the total atom density in the beam): odd levels $4f^{11}6s^2^4I^o$, $J = 15/2(0) - 99.27\%$, $13/2(5419) - 0.57\%$, $11/2(8605) - 0.026\%$, $9/2(10696) - 0.0032\%$; even levels $4f^{10}(^5I_8)5d_{3/2}6s^2(8,3/2)$, $J = 17/2(8378) - 0.048\%$, $15/2(8427) - 0.042\%$, $13/2(9147) - 0.019\%$, $19/2(9741) - 0.015\%$. The energy levels in inverse centimetres are given in parentheses. Therefore, the total population of the even levels is 0.114%; i. e., it is three orders of magnitude smaller than the total population of the odd levels.

The actual population of the low-lying excited levels under discussion is likely to be lower than the estimates given above: when atoms are evaporated into a vacuum from an open surface, the equilibrium population is usually not reached and, moreover, there occurs some selectivity in the level distribution. The excitation in our experiment is effected virtually from the single ground level because its population accounts for more than 99% of the total number of atoms in the beam.

When studying the most intense resonance lines of Ho I, the atom density was lowered to 10^9 cm^{-3} to minimise reabsorption. However, this is insignificant for the lines discussed in this work, since their excitation cross sections are comparatively small and, which is most important, there are no resonance transitions among the ones under study. The current density of the electric beam did not exceed 0.8 mA cm^{-2} in the operating energy range. The width of the distribution of the electron energy was 0.9 eV for an energy of 100 eV and 1.0 eV for energies of 20 and 200 eV (for 90% of the electrons). The actual spectral resolution was $\sim 0.1 \text{ nm}$ for $\lambda \leq 600 \text{ nm}$ and about 0.25 nm in the longer-wavelength

range. The remaining experimental conditions are typical of the investigations involving extended beams [16, 17].

3. Results and discussion

The results obtained for the odd levels of Ho I are presented in Table 1. The lines should satisfy one of the following criteria: (i) availability of the OEF, (ii) appartenance of the upper level to the $4f^{11}5d6s$ configuration, (iii) availability of the information on the term of the upper level (and not only on the configuration). The $4f^{11}5d6s$ configuration is set off because the 22014 cm^{-1} laser level of atomic holmium refers to precisely this configuration. Table 1 gives the wavelength λ , the transition and the inner quantum number J , the lower (E_{low}) and upper (E_{up}) energy levels, the excitation cross sections for an energy of 50 eV Q_{50} and at the peak of the OEF Q_{max} , the location of the OEF peak $E(Q_{\text{max}})$, and the OEF numbers in accordance with their numbering in Fig. 2. The line parameters determined or classified in present work are enclosed in parentheses. The classification procedure was conducted employing the information on Ho I levels borrowed from Ref. [7], in some cases complemented by the more extensive data of Ref. [8]. In four cases there occurs blending, three blending lines being unclassified. In all four cases, the available information is insufficient for separating the blends.

From Table 1 it follows that the efficiency of excitation of the levels whose parity coincides with the parity of the ground state is relatively low. For the majority of the levels investigated, there occurs a competition of radiative transitions, i.e., branching. The measured Q_{50} values lie in the range $(0.09 - 4.96) \times 10^{-18}\text{ cm}^2$, whereas for most intense resonance lines they exceed 10^{-16} cm^2 . Among the lines investigated are two transitions from the 22014 cm^{-1} laser level located in the red spectral region. However, the laser transition was not recorded directly, because it resides in the IR region, outside the operating spectral range of the facility.

The energy diagram of atomic holmium is shown in Fig. 3; all known configurations of Ho I are shown. The arrows depict all groups of the interconfiguration transitions

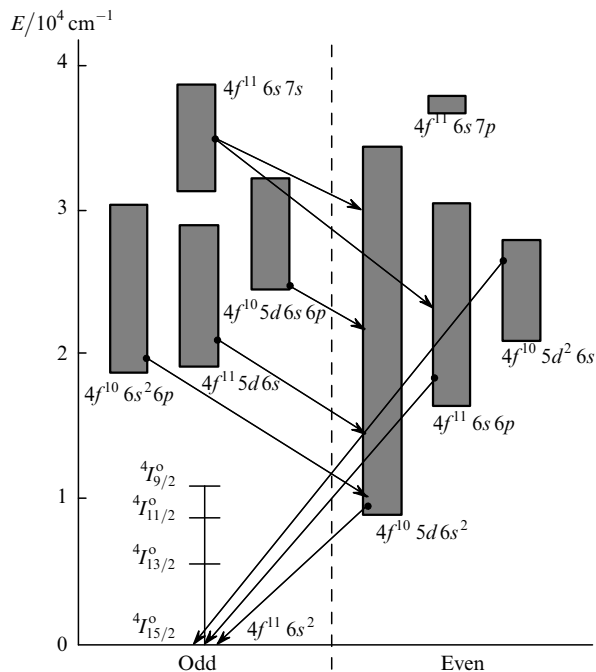


Figure 3. Energy level diagram for all known configurations of atomic Ho I.

for which the excitation cross sections were measured by the author in studies of inelastic electron collisions with holmium atoms. However, of the group of transitions from the levels of odd configurations, the $4f^{10}6s^26p \rightarrow 4f^{10}5d6s^2$ transitions were beyond the scope of this work. All the excitation cross sections for the transitions of this group proved to be comparatively small, with the effect that none of the OEFs were recorded.

The majority of spectral lines under investigation are related to the allowed single-electron $7s \rightarrow 6p$ and $6p \rightarrow 6s$ transitions. However, as noted in Section 1, there also occur transitions involving a more complex rearrangement of the

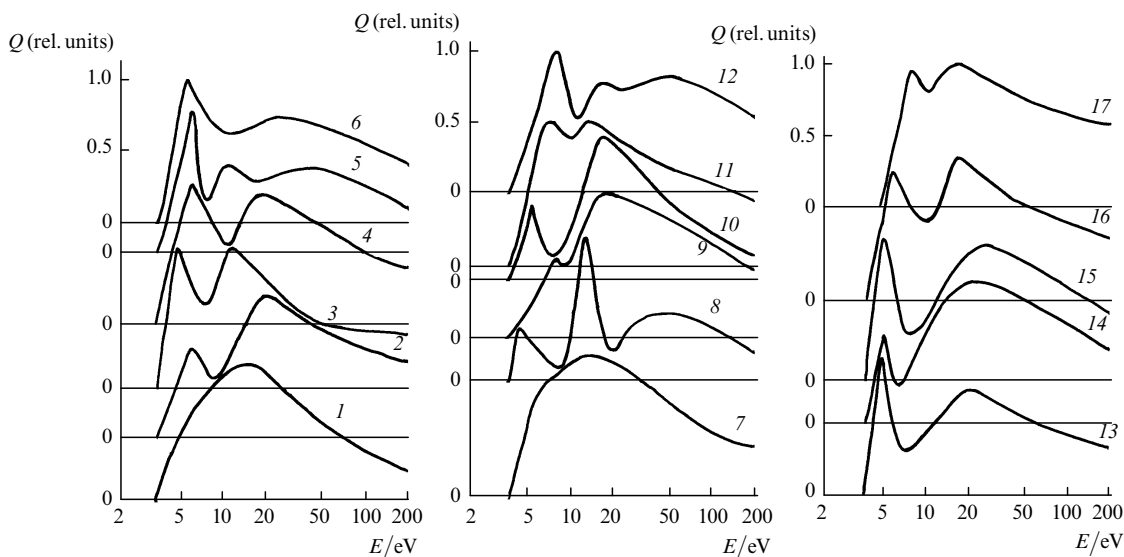


Figure 2. Optical excitation functions of the transitions from odd levels of Ho I, normalised to unity at the maximum and having individual origins in the ordinate axis.

Table 1. Excitation cross sections of atomic holmium (transitions from odd levels).

λ (nm)	Transition	J	E_{low} cm ⁻¹	E_{up} cm ⁻¹	$\frac{Q_{50}}{10^{-18} \text{ cm}^2}$	$\frac{Q_{\text{max}}}{10^{-18} \text{ cm}^2}$	$\frac{E(Q_{\text{max}})}{\text{eV}}$	OEF No.		
383.730	$4f^{10}5d6s^2(7, 3/2) - 4f^{11}6s7s(13/2, 0)^\circ$	13/2 – 13/2	12344	38397	1.12	1.50	16	17		
406.757	$4f^{10}5d6s^2(8, 3/2) - 4f^{11}6s7s(15/2, 0)^\circ$	15/2 – 15/2	8427	33005	1.40	–	–	–		
406.805	–	–	–	–						
419.024	$4f^{10}5d6s^2(8, 3/2) - 4f^{11}6s7s(15/2, 0)^\circ$	13/2 – 15/2	9147	33005					2.45	–
432.534	$4f^{10}5d6s^2(8, 3/2) - 4f^{10}5d6s6p^\circ$	15/2 – 15/2	8427	31540	0.57	0.71	5.0	15		
433.403	$4f^{10}5d6s^2(8, 3/2) - 4f^{11}6s7s(15/2, 1)^\circ$	17/2 – 15/2	8378	31443	0.80	0.94	25	14		
441.004	$4f^{10}5d6s^2(8, 3/2) - 4f^{11}6s7s(15/2, 1)^\circ$	13/2 – 13/2	9147	31816	0.26	–	–	–		
441.578	$4f^{10}5d6s^2(8, 3/2) - 4f^{10}5d6s6p^\circ$	17/2 – 19/2	8378	31018	1.21	1.51	8.0	12		
446.409	$4f^{10}5d6s^2(8, 3/2) - 4f^{10}5d6s6p^\circ$	17/2 – 15/2	8378	30773	1.38	2.08; 2.08	7.2; 14	11		
454.252	$4f^{10}5d6s^2(8, 3/2) - 4f^{10}5d6s6p^\circ$	15/2 – 13/2	8427	30339	0.19	0.23	17	9		
462.822	$(4f^{10}5d6s^2(8, 3/2) - 4f^{10}5d6s6p^\circ)$	17/2 – 15/2	8378	29979	0.09	0.14	6.0	6		
467.711	$4f^{10}5d6s^2(8, 3/2) - 4f^{11}6s7s(15/2, 1)^\circ$	19/2 – 17/2	9741	31116	0.30	0.58	5.0	13		
469.050	$4f^{10}5d6s^2(8, 3/2) - 4f^{10}5d6s6p^\circ$	17/2 – 19/2	8378	29692	0.36	0.61	6.4	5		
469.857	$4f^{10}5d6s^2(8, 3/2) - 4f^{10}5d6s6p^\circ$	19/2 – 19/2	9741	31018	0.29	0.36	8.0	12		
471.752	$4f^{10}5d6s^2(8, 3/2) - 4f^{10}5d6s6p^\circ$	13/2 – 13/2	9147	30339	1.10	1.33	17	9		
478.292	$4f^{10}5d6s^2(8, 3/2) - 4f^{11}5d6s^\circ$	13/2 – 15/2	9147	30049	3.66	5.38	14	7		
479.887	$(4f^{10}5d6s^2(8, 3/2) - 4f^{10}5d6s6p^\circ)$	13/2 – 15/2	9147	29979	0.40	0.61	6.0	6		
483.745	$4f^{10}5d6s^2(8, 5/2) - 4f^{11}6s7s(15/2, 0)^\circ$	15/2 – 15/2	12339	33005	0.30	–	–	–		
490.208	$4f^{10}5d6s^2(8, 3/2) - 4f^{10}5d6s6p^\circ$	19/2 – 17/2	9741	30135	0.31	0.67	13	8		
492.598	$4f^{10}5d6s^2(8, 5/2) - 4f^{10}5d6s6p^\circ$	19/2 – 17/2	11689	31984	0.55	0.82	16	16		
504.473	$4f^{10}5d6s^2(8, 3/2) - 4f^{10}5d6s6p^\circ$	15/2 – 17/2	8427	28244	0.83	1.84; 1.84	5.0; 12	3		
508.878	$4f^{10}5d6s^2(8, 5/2) - 4f^{10}5d6s6p^\circ$	15/2 – 17/2	12339	31984	0.25	0.37	16	16		
510.436	$4f^{10}5d6s^2(8, 5/2) - 4f^{11}6s7s(15/2, 1)^\circ$	17/2 – 17/2	11530	31116	0.51	0.98	5.0	13		
511.513	$4f^{10}5d6s^2(8, 3/2) - 4f^{10}5d6s6p^\circ$	17/2 – 17/2	8378	27923	0.55	0.72	20	2		
512.781	$(4f^{10}5d6s^2(8, 3/2) - 4f^{10}5d6s6p^\circ)$	15/2 – 17/2	8427	27923	0.55	0.72	20	2		
513.965	$4f^{10}5d6s^2(8, 3/2) - 4f^{11}5d6s^\circ$	13/2 – 13/2	9147	28598	0.32	0.47	6.4	4		
519.523	$(4f^{10}5d6s^2(8, 5/2) - 4f^{10}5d6s6p^\circ)$	17/2 – 15/2	11530	30773	0.19	0.29; 0.29	7.2; 14	11		
521.711	$4f^{10}5d6s^2(8, 5/2) - 4f^{10}5d6s6p^\circ$	21/2 – 21/2	11322	30484	1.01	1.94	17	10		
523.300	$4f^{10}5d6s^2(8, 5/2) - 4f^{11}6s7s(15/2, 1)^\circ$	15/2 – 15/2	12339	31443	0.32	0.38	25	14		
523.325	$4f^{10}5d6s^2(8, 5/2) - 4f^{10}5d6s6p^\circ$	21/2 – 19/2	11322	30425					–	–
531.924	$(4f^{10}5d6s^2(8, 5/2) - 4f^{10}5d6s6p^\circ)$	19/2 – 21/2	11689	30484					17	10
531.965	–	–	–	–	0.20	0.38	–	–		
537.347	$4f^{10}5d6s^2(8, 5/2) - 4f^{10}5d6s6p^\circ$	17/2 – 17/2	11530	30135	0.63	1.37	13	8		
548.169	$4f^{10}5d6s^2(8, 3/2) - 4f^{10}5d6s6p^\circ$	15/2 – 17/2	8427	26664	0.59	1.05	14	1		
549.857	$(4f^{10}5d6s^2(8, 3/2) - 4f^{10}5d6s6p^\circ)$	19/2 – 17/2	9741	27923	0.42	0.55	20	2		
550.451	$(4f^{10}5d6s^2(8, 5/2) - 4f^{10}5d6s6p^\circ)$	17/2 – 19/2	11530	29692	0.55	0.93	6.4	5		
555.314	$(4f^{10}5d6s^2(8, 5/2) - 4f^{10}5d6s6p^\circ)$	19/2 – 19/2	11689	29692	0.25	0.42	6.4	5		
561.684	$4f^{10}5d6s^2(8, 3/2) - 4f^{11}5d6s^\circ$	15/2 – 13/2	8427	26225	0.24	–	–	–		
582.190	$(4f^{10}5d6s^2(8, 5/2) - 4f^{11}5d6s^4L^\circ)$	19/2 – 17/2	11689	28861	0.53	–	–	–		
605.071	$(4f^{10}5d6s^2(8, 5/2) - 4f^{11}5d6s^4L^\circ)$	15/2 – 17/2	12339	28861	1.16	–	–	–		
646.709	$4f^{10}5d6s^2(8, 3/2) - 4f^{11}5d6s^4K^\circ$	15/2 – 17/2	8427	23885	4.96	–	–	–		
655.097	$4f^{11}6s6p(15/2, 0) - 4f^{11}6s7s(15/2, 1)^\circ$	15/2 – 17/2	15855	31116	1.53	2.94	5.0	13		
669.432	$4f^{11}6s6p(15/2, 1) - 4f^{11}6s7s(15/2, 1)^\circ$	15/2 – 13/2	16882	31816	0.58	–	–	–		
677.468	$4f^{11}6s6p(15/2, 1) - 4f^{11}6s7s(15/2, 1)^\circ$	13/2 – 13/2	17059	31816	0.51	–	–	–		
678.543	$4f^{11}6s6p(15/2, 1) - 4f^{11}6s7s(15/2, 1)^\circ$	17/2 – 15/2	16709	31443	0.97	1.14	25	14		
681.104	$4f^{10}5d6s^2(7, 5/2) - 4f^{11}6s7s(15/2, 1)^\circ$	17/2 – 17/2	16438	31116	2.03	3.90	5.0	13		
686.585	$4f^{11}6s6p(15/2, 1) - 4f^{11}6s7s(15/2, 1)^\circ$	15/2 – 15/2	16882	31443	0.81	0.95	25	14		
693.949	$4f^{11}6s6p(15/2, 1) - 4f^{11}6s7s(15/2, 1)^\circ$	17/2 – 17/2	16709	31116	1.30	2.50	5.0	13		
733.193	$4f^{10}5d6s^2(8, 3/2) - 4f^{11}5d6s^\circ$	17/2 – 15/2	8378	22014	2.36	–	–	–		
758.920	$4f^{10}5d6s^2(8, 3/2) - 4f^{11}5d6s^\circ$	17/2 – 17/2	8378	21552	1.85	–	–	–		
759.187	–	–	–	–						
776.965	$4f^{10}5d6s^2(8, 3/2) - 4f^{11}5d6s^\circ$	13/2 – 15/2	9147	22014					2.73	–
761.705	$4f^{10}5d6s^2(8, 3/2) - 4f^{11}5d6s^\circ$	15/2 – 17/2	8427	21552	2.29	–	–	–		
781.548	$4f^{11}6s6p(15/2, 2) - 4f^{11}6s7s(15/2, 1)^\circ$	15/2 – 15/2	18651	31443	1.89	2.22	25	14		

Odd		Even				
$4f^{11} 6s^2$	$4f^{11} 5d6s$	$4f^{10} 5d6s^2$			$4f^{11} 6s6p$	$4f^{10} 5d^2 6s$
$4I^o$	$4I^o$	$5I_5$	$5I_2$	$5I_8$	$4I_{13/2}^o$	$5I$
		(5, 5/2)	(7, 3/2)	(8, 5/2)	(13/2, 1)	(13/2, 1)
					(13/2, 0)	

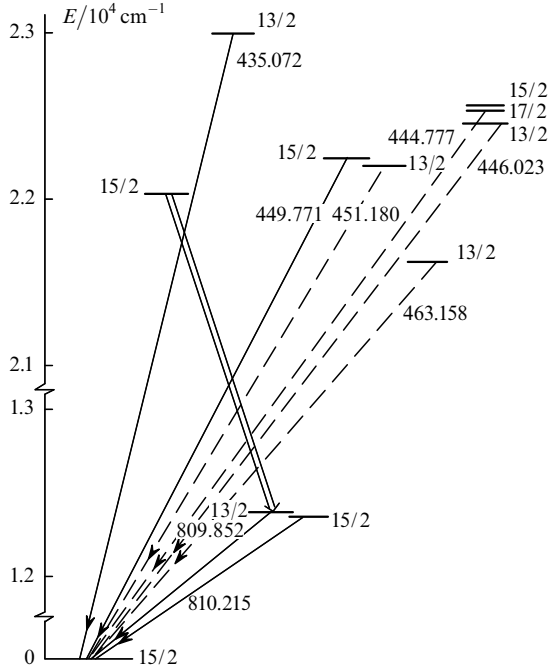


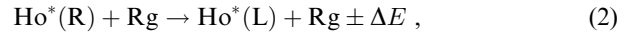
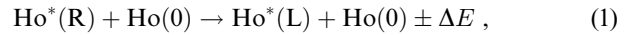
Figure 4. Simplified energy level diagram of atomic holmium. The double arrow indicates the laser transition, a fractional number by an level denotes the total momentum, and a number by an arrow indicates the wavelength of the spectral line in nanometres; the lines first investigated in this work are indicated by dashed arrows.

electron shell, $4f \rightarrow 6s$ and $4f 7s \rightarrow 5d 6s$, which are afforded primarily by the configuration mixing. At the same time, the collisions involving electron exchange are supposedly of considerable importance in the excitation of the levels of odd configurations. The shape of the OEFs shown in Fig. 2 is indirect evidence of this. Except for the OEFs No. 1 and 7, all of them have a sharp peak in the near-threshold energy region typical of collisions involving replacement of one of the atomic shell electrons with the incident electron.

Table 2. Excitation cross sections of atomic holmium (transitions from even levels).

λ nm	Upper level	Composition (%)		J	E_{low} cm^{-1}	E_{up} cm^{-1}	Q_{50} $10^{-18}cm^2$	Q_{max} $10^{-18}cm^2$	$E(Q_{max})$ eV	OEF No.
		main component	main admixture							
435.073	$4f^{10} (5I_5) 5d_{5/2} 6s^2 (5, 5/2)$	41 ($5I$) $4K$		15/2 – 13/2	0	22978	32.0	40.0	19	3
(695.556)	$4f^{10} (5I_5) 5d_{5/2} 6s^2 (5, 5/2)$	41 ($5I$) $4K$		11/2 – 13/2	8605	22978	0.90	1.13	19	3
(444.777)	$4f^{10} (5I) 5d^2 (3F) (7K) 6s$	22 $8K$	18 ($5I$) ($3F$) ($7H$) $8H$	15/2 – 17/2	0	22476	0.81	–	–	–
(446.023)	$4f^{10} (5I) 5d^2 (3F) (7F) 6s$	24 $8F$	20 ($5I$) ($3F$) ($7H$) $8H$	15/2 – 13/2	0	22414	0.52	–	–	–
449.771	$(4f^{11} 4I_{13/2}^o) 6s6p (3P_1^o) (13/2, 1)$	43 ($4I^o$) ($3P^o$) $6K$		15/2 – 15/2	0	22227	1.61	1.75	20	2
594.803	$(4f^{11} 4I_{13/2}^o) 6s6p (3P_1^o) (13/2, 1)$	43 ($4I^o$) ($3P^o$) $6K$		13/2 – 15/2	5419	22227	2.58	2.80	20	2
(451.180)	$4f^{11} (4I_{13/2}^o) 6s6p (3P_1^o) (13/2, 1)$			15/2 – 13/2	0	22157	0.82	–	–	–
597.276	$(4f^{11} 4I_{13/2}^o) 6s6p (3P_1^o) (13/2, 1)$			13/2 – 13/2	5419	22157	6.18	–	–	–
597.352	$4f^{10} 5d 6s^2$	70	30 $4f^{11} 6s6p$	15/2 – 13/2	0	16735				
(463.158)	$(4f^{11} 4I_{13/2}^o) 6s6p (3P_0^o) (13/2, 0)$			15/2 – 13/2	0	21584	1.31	1.49	6.0	1

When discussing the possible mechanisms of formation of the population inversion in a holmium vapour laser, Gerasimov [6] arrived at the conclusion that the following processes are most probable:



where $Ho^*(R)$, $Ho^*(L)$, and $Ho(0)$ are holmium atoms respectively in the resonance, upper laser, and ground levels; Rg is an atom of the inert gas; and ΔE is the energy difference between the levels exchanging the excitation.

Fig. 4 reproduces Fig. 2 from Ref. [6]. It shows a part of the level diagram of atomic holmium, which comprises the laser levels and the levels presumably participating in the formation of population inversion. The difference ΔE between the selected energy levels and the upper laser level falls within the range from 143 to 964 cm^{-1} . Gerasimov [6] regretfully noted that electron-impact excitation cross sections are known [14] only for two of the lines having the upper level given in Fig. 4. In the present work, the excitation cross sections were measured for the transitions from the remaining levels, with the exception of the $4f^{10} (5I) 5d^2 (3F) (7G) 6s_{15/2}$ level with an energy of 22500.62 cm^{-1} . The corresponding resonance transitions are shown by dashed lines in Fig. 4.

The results of measurements for these levels are presented in Table 2. All the transitions included in Table 2 terminate in the levels of the ground term with $J = 15/2$ (0), 13/2 (5419), and 11/2 (8605). Apart from the quantities given in Table 1, also given in Table 2 is the content of the main component and the leading admixture for the upper levels (according to the data of Ref. [7]); the OEFs are shown in Fig. 5. Apart from resonance transitions, three transitions to higher levels of the fundamental term were also recorded. The 597.276 and 597.352 nm lines are blended; however, it is impossible to decide between them on a basis of the presently available information. It is pertinent to note that the excitation cross sections of the 435.072 and 449.771 nm lines measured in this work are on the average 3.22 times larger than those given in Ref. [14].

References

1. Cahuzac Ph Phys. Lett. A **27** 473 (1968)
2. Cahuzac Ph Phys. Lett. A **31** 541 (1970)

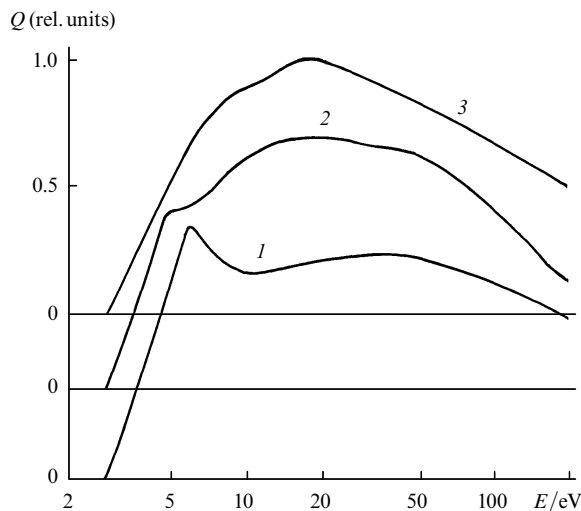


Figure 5. Optical excitation functions for the transitions from even levels of Ho I.

3. Handbook of lasers with selected data on optical technology (Cleveland, Chemical Rubber Co, 1971)
4. Radtsig A A, Smirnov B M Reference Data on Atoms, Molecules, and Ions (Berlin: Springer-Verlag, 1985)
5. Zaidel' A N, Ostrovskaya G V, Ostrovskii Yu I Tekhnika i Praktika Spektroskopii (Techniques and Practice of Spectroscopy) (Moscow: Nauka, 1972) p. 345
6. Gerasimov V A Opt. Spektrosk. **87** 156 (1999) [Opt. Spectrosc. **87** 144 (1999)]
7. Martin W C, Zalubas R, Hagan L Atomic Energy Levels. The Rare-Earth Elements (Washington: NBS-US, 1978) p. 296
8. Wyart J-F, Camus P, Verges J Physica C **92** 377 (1977)
9. Childs W J, Cock D R, Goodman J S J. Opt. Soc. Am. **73** 151 (1983)
10. Smirnov Yu M Spectrochim. Acta, Part B **49** 469 (1994)
11. Corliss C H, Bozman W R Experimental Transition Probabilities for Spectral Lines of Seventy Elements (Washington, D.C.: U.S. Government Printing Office, 1962, p.153)
12. Gorshkov V N, Komarovskii V A Opt. Spektrosk. **47** 631 (1979)
13. Worm T, Shi P X, Poulsen O Phys. Scr. **42** 569 (1990)
14. Bodylev A Yu, Krasavin A Yu, Smirnov Yu M Opt. Spektrosk. **57** 983 (1984)
15. Van Zyl B, Dunn G H, Chamberlain G, Heddle D W O Phys. Rev. A **22** 1916 (1980)
16. Smirnov Yu M Zh. Prikl. Spektrosk. **57** 23 (1992) [J. Appl. Spectrosc. **57** 545 (1992)]
17. Smirnov Yu M J. Phys. II **4** 23 (1994)